INSTITUTE OF PHYSICS PUBLISHING JOURNAL OF MICROMECHANICS AND MICROENGINEERING

J. Micromech. Microeng. **16** (2006) 1416–1423 doi:10.1088/0960-1317/16/7/040

Inline-actuated suspension for the fine head positioning of HDD

Gih Keong Lau[1] **and Hejun Du**[2]

[1] Delft University of Technology, Faculty of Mechanical, Maritime and Material Engineering, Mekelweg 2, 2628 CD Delft, The Netherlands
[2] Nanyang Technological University, School of Mechanical and Aerospace Engineering, Nanyang Avenue, Singapore 639798

E-mail: gihkeong@yahoo.com

Received 10 March 2006, in final form 16 May 2006
Published 8 June 2006
Online at stacks.iop.org/JMM/16/1416

Abstract

A new design of inline-actuated suspension is developed for application in the dual-stage head positioning of hard disk drives (HDD). This design exploits a parallel mechanism to convert longitudinal piezoelectric actuation into a lateral stroke. It is embodied in an elongated portion of a slender load beam. Besides serving the intended function of adequate stroke, the new design significantly improves shock resistance and dynamics. Its sway frequency improves by 19%, as compared to a push–pull design. In addition, the piezoelectric plate for inline actuation is subjected to 66% less shock-induced stress than the pair for push–pull actuation. The new actuator only requires standard manufacturing and assembly processes for realization and no costly miniaturization.

(Some figures in this article are in colour only in the electronic version)

1. Introduction

Over the past decades, many dual-stage milli- and micro-actuators have been developed to implement fine head positioning of hard disk drives. They can be divided into three categories according to the deployed positions: (1) the suspension level; (2) the slider level; (3) the head level. Among these, the actuators on the slider level and the head level are best for collocated controls. The actuators on the suspension level are non-collocated and thus their performances are more influenced by the suspension dynamics [1]. Though the actuated suspensions are not the best technology for ultra-high density disk drive, their performance suffices the applications in the disk drive of very high density. In addition, they can be produced at a lower cost given the existing manufacturing process and equipments. As such, they are going to be commercialized sooner than the other two rival technologies.

There are two major means of driving a suspension: piezoelectric and electromagnetic actuators. But piezoelectric actuation is more widely adopted. In an early design by Mori *et al* [2], a single piezoelectric stack was deployed at the tip of a rotary arm and aligned laterally so as to bring a magnetic head at the distal end of the assembly into a cross-track motion. However, the piezoelectric stack is of considerable length and cannot be fitted into a slender suspension of limited width. Subsequent designs of actuated suspensions are developed mostly based on a push–pull principle (see figure 1(*a*)). The driving principle is based on two piezoelectric plates located at the root of suspension, one moving forward and the other moving backward simultaneously in order to swing a magnetic head. The piezoelectric plates can operate on either an extension mode [3, 4] or a shear mode [5]. These designs are well developed and almost ready for commercial application. But they need further improvement to meet the requirements of disk drives for higher capacity and higher speed.

As the data density on a disk increases, a track pitch between magnetic data decreases but the accuracy of head positioning increases. Hence, a full stroke need not be as large as an initial specification. For example, a piggyback actuator developed in the early 90s had to achieve a full stroke of ± 2.3 μm at a supplying voltage of 100 V for covering three tracks at data density of 17 kTPI [2]. A subsequent piggyback actuator was developed to achieve a full stroke of ± 1.0 μm at a lower voltage for data density of 25 kTPI [6]. With advances in control methods, an even finer stroke of ± 0.45 μm suffices to correct positioning error for a disk drive of 13.5 kTPI [7].

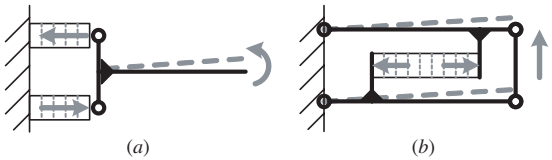

Figure 1. Driving mechanisms using piezoelectric actuators: (*a*) conventional push–pull actuation; (*b*) novel inline actuation.

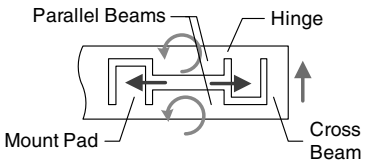

Figure 2. Embodiment of inline actuation: expansive forces drive two mounting pads apart such that the parallel beams of suspension rotate counter-clockwise and bring a cross beam laterally upward.

Meanwhile, the sway resonance frequencies of the actuators improved from 6 kHz [2] to 9.0 kHz [7] over generations of design evolution.

Besides the increasing capacity, a faster data access is another important design trend for the disk drives, in particular for enterprise server applications. The enterprise disk drives operate at higher rotating speeds, for example 10k rpm or 15k rpm, as compared to 7.2k rpm for the personal storage. When the disk is rotating at such a high speed, other implications happen to affect the accuracy of head positioning. For example, a fast spinning disk may induce turbulent air disturbance, which excites the disk into fluttering or the suspensions into unduly vibration [8, 9]. If the suspensions do not have a high enough mechanical resonant frequency, the head positioning accuracy will be compromised even though it is assisted with the dual-stage actuation. Thus, a successful actuated suspension should possess attributes of a high lateral or sway resonant frequency as well as an adequate stroke. However, most reported designs have limited resonant frequencies, which are generally compromised by in-plane flexibility for actuation mechanism [4].

Since the prior designs cannot meet the demand for higher dynamic performance, redesign of the actuated suspensions is generally expected. To meet specifications for a 100 kTPI capacity, a new design has to achieve a lateral resonant frequency higher than 10 kHz and an adequate stroke [4]. Dynamics of the actuated suspensions are influenced by two main factors: (1) the profile of the component load beam and (2) the mechanism design of the driving actuator. The profile of component load beam can be optimized for enhanced dynamics using topology optimization [10]. On the other hand, the performance of the actuating mechanism mainly depends on the kinematics enumeration. If the kinematics design is fixed, the room to enhance the dynamics of the mechanism is rather limited. For example, thickening pivotal hinges for a push–pull actuator could improve mechanism dynamics to certain extent, but it does not serve well to generate the lateral stroke.

To further enhance dynamic performance, piezoelectric elements are preferably miniaturized and deployed on the elongated portion of the suspension, which is located closer to a slider. The closer actuator placement may bring benefits of the near-collocated control by avoiding interference of the suspension dynamics. However, the push–pull actuator comprising of two piezoelectric plates cannot be fit into the limited room of the elongated suspension. To fit into the limited room without involving costly miniaturization, an alternative actuating mechanism using a single piezoelectric plate is to be sought.

This paper proposes a novel design of actuated suspension, which deploys a single piezoelectric plate on the elongated portion of a suspension. The piezoelectric plate is aligned along the centerline of the elongated suspension and actuates a parallel mechanism, which converts a longitudinal stroke into a lateral cross-track motion (see figure 1(*b*)). Thus, it is termed as an inline actuation. We briefly presented the driving concept in the INTERMAG 2005 conference [11]. Here, we present a full account of the novel actuator design, together with a parametric study on the design.

2. A novel design

Inline actuated suspension consists of a load beam embodied with a parallel mechanism and a piezoelectric plate. The parallel mechanism comprises two parallel beams (figure 2). Each of the parallel beams has a mounting tab: one has it at a proximal end while the other has it at a distal end. The ends of the parallel beams are connected together through a cross beam. The middle of the two parallel beams is widened, filling the gap between the two mounting tabs. The widened beam sections serve to increase in-plane stiffness. A slit of complicated shape is formed by the inner sides of the parallel beams, the mounting tabs and the cross beam; whereas flanks of the elongated suspension are defined by the outer sides of the parallel beams.

The piezoelectric plate spans between the two mounting tabs: each end of the plate is lapped onto the tabs. It is polarized across thickness. When a potential difference is applied across its thickness, the plate will expand and thus push the two mounting tabs apart. The longitudinal expansion will then induce a counter-clockwise rotation to the two parallel beams, which bring the cross beam into a laterally upward motion.

Beside the in-plane actuation, there will be a coupled out-of-plane motion at the tip of suspension because the piezoelectric plate is lapped on one side of the suspension, causing thickness asymmetry. In addition, the mounting tabs that are asymmetrically located with respect to the parallel beams may cause twisting when actuated in-plane. It is possible to remove the thickness asymmetry. Lapping two plates onto both sides of load beams can effectively produce a symmetric design across thickness. But, in this context, the single plate lapping on one side is considered due to the concerns over material and assembly cost. A full assembly of such an inline-actuated suspension is shown in figure 3.

The present design embodied a motion conversion mechanism different from the push–pull design (see figure 1). It requires a single plate for actuation, rather than two as for the push–pull design. It is thus more economical. The single piezoelectric plate deployed on the elongated portion is less likely to interfere with a spring region. Moreover,

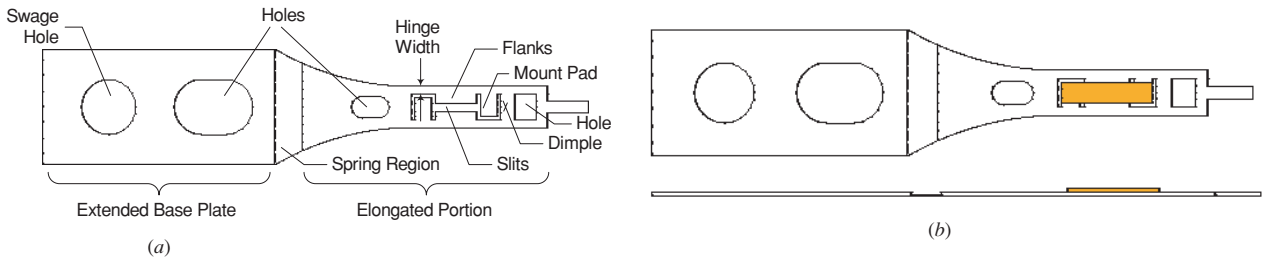

Figure 3. An inline-actuated suspension: (*a*) its load beam; (*b*) its assembly with a piezoelectric plate.

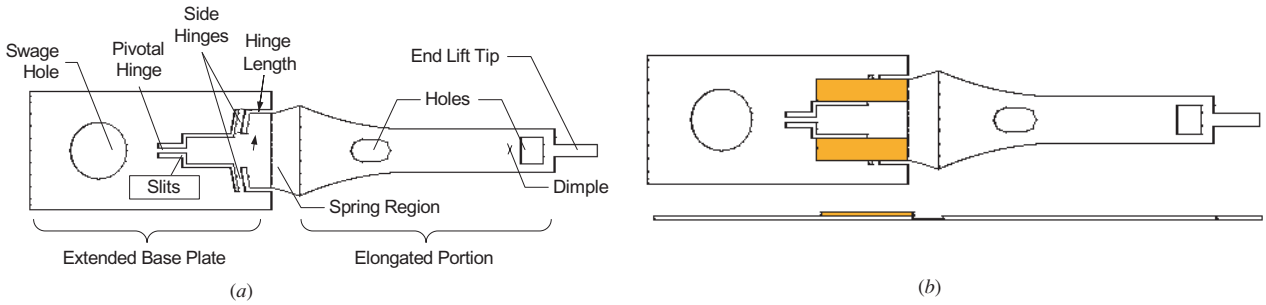

Figure 4. A push–pull actuated suspension: (*a*) its load beam; (*b*) its assembly with two piezoelectric plates.

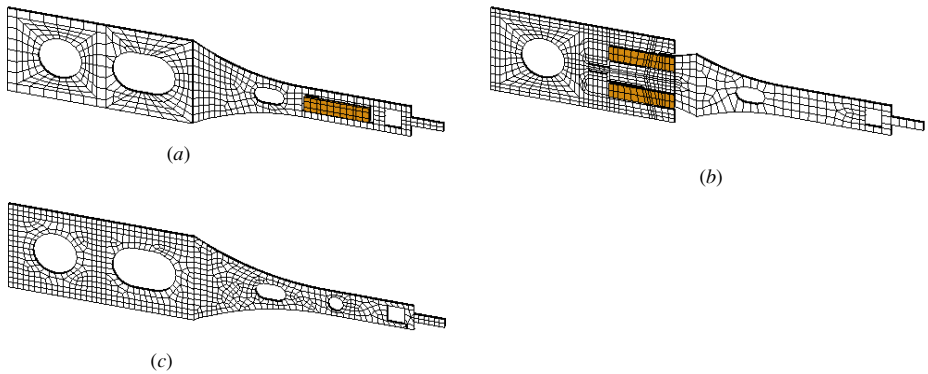

Figure 5. Finite element models for suspension assemblies: (*a*) an inline-actuated suspension; (*b*) a push–pull actuated suspension; (*c*) a bare suspension.

the piezoelectric element on the inline-actuated suspension is better protected against a high shock and less prone to damages. In contrast, the piezoelectric elements for the push–pull design as shown in figure 4 are more likely to interfere with the spring region given their adjacency, and they are more susceptible to damage given the limited out-of-plane stiffness of pivotal and side hinges.

3. Finite element simulation

3.1. Modeling

Finite element simulation is performed to predict and verify the performance of the newly designed actuated suspension. Figure 5(*a*) shows a finite element mesh of the inline-actuated suspension. For comparison, a prior design of push–pull actuated suspension (figure 5(*b*)) and a bare load beam (figure 5(*c*)) are also simulated. Both static and dynamic analyses are performed to determine performance characteristics of the actuated suspension designs. The simulation is done using commercial finite element software, ANSYS. The finite element models are constructed using SOLID45 elements for modeling the stainless steel suspension (also termed as load beam) and the cured epoxy adhesive, and SOLID5 elements for modeling the piezoelectric materials. The material properties in use are given in tables 1, 2 and 3.

Table 1. Properties used for piezoelectric ceramics [12].

Piezoelectric constant	
d_{31}	-340×10^{-12} (m V^{-1})
d_{33}	645×10^{-12} (m V^{-1})
Elastic modulus	
C_{11}^{E}	12×10^{10} (N m^{-2})
$C_{12}^{E} = C_{13}^{E}$	7.7×10^{10} (N m^{-2})
C_{33}^{E}	11.4×10^{10} (N m^{-2})
C_{55}^{E}	2.1×10^{10} (N m^{-2})
Poisson's ratio σ	0.37
Density, ρ	7800 (kg m^{-3})

Table 2. Properties used for stainless steel.

Young's modulus	193.0 GPa
Poisson's ratio	0.30
Density	8030 kg m^{-3}

Table 3. Properties used for cured epoxy [13].

Young's modulus	1.3 GPa
Poisson's ratio	0.36
Density	2120 kg m^{-3}

These designs are modeled with a load beam of almost equal dimensions, except a difference in the intricate mechanisms for piezoelectric actuation. The common dimensions are adopted for the extended base and the elongated load beam so that a fair comparison can be done to show the effects of actuation mechanisms without being influenced by the load beam design. The common dimensions are as follows. The load beam has a thickness of 0.1 mm, an extended base plate of 4.2 mm wide and 8.0 mm long, a dimple to swage hole length of 14.5 mm and a half-etched spring region of 1 mm long and 0.05 mm thick. The distal end of the elongated load beam is 1.5 mm wide and is equipped with an end lift tip for the purpose of load–unload. Depending on the design, the actuated load beams carry one or two pieces of piezoelectric plates, which are cut into a dimension of 3 mm long and 0.70 mm wide and 0.10 mm thick.

A clamped-free boundary condition is imposed to the actuated suspension in all simulation. This condition describes the configuration of the suspension assembly before being loaded onto the disk drives. Four weld points, around the swage hole, and the swage hole itself are fully fixed while other portions of the load beam are free to move. In addition to the boundary condition, loading conditions are imposed in different analyses. A driving voltage of 30 V is applied to the electrode of the piezoelectric plate for static analysis. A sinusoidal voltage at 30 V over a range of frequencies is imposed to the assemblies for predicting frequency responses. Various out-of-plane static accelerations are imposed to the assemblies for quasi-shock analysis.

3.2. Results and discussions

Table 4 summarizes simulated performances of the actuated suspensions, as well as a reference of the bare load beam (figure 5). The inline-actuated suspension has a spring rate comparable to that of the bare load beam; whereas the push–pull actuated suspension has a slightly higher spring rate. However, the inline-actuated suspension achieves a lower static lateral stroke of 0.33 μm at 30 V, as compared to 1.01 μm obtained by the push–pull actuated suspension at the same voltage. On dynamics, both actuated suspensions generally have reduced resonant frequencies as compared to the bare load beam. However, the inline-actuated suspension still possesses good dynamic performance. For example, the inline-actuated suspension has higher first torsional and first sway frequencies at 6.24 kHz and 10 kHz, respectively; whereas, the push–pull actuated suspension has lower torsional and sway frequencies, at 5.86 kHz and 8.43 kHz, respectively. The new design

Table 4. Performance comparisons among actuated suspensions and a bare load beam.

	A bare load beam	A push–pull actuator	An inline actuator
Lateral stroke @ 30 V	–	1.01	0.33
Cantilever frequency (kHz)	0.44	0.47	0.42
1st torsion frequency (kHz)	6.33	5.86	6.24
2nd torsion frequency (kHz)	13.02	12.22	12.35
1st sway frequency (kHz)	14.94	8.43	10.06
Spring rate (N m^{-1})	41.72	48.34	41.03

improves the sway frequency by 19% higher than the push–pull actuator.

When subjected to an out-of-plane shock acceleration, an inertial force is induced to both the load beam and the piezoelectric ceramics. The inline-actuated suspension carries a single piezoelectric plate with strong parallel flexures (having 0.30 mm wide hinge and 0.5 mm wide flanks). On the contrary, the push–pull actuated suspension carries two plates on three flexible pivotal hinges of 0.2 mm width. Figure 6 shows stress distributions on two types of actuated suspensions under a 100 G static acceleration. The stress contours show that the single piezoelectric plate for the inline-actuated suspension is away from the highly stressed spring region; whereas, the pair for the push–pull actuated suspension are closer to the highly stressed region. Under all range of static accelerations (see figure 7), the piezoelectric plate for the inline-actuated suspensions is found to be subjected to 66% less the maximum stress than the pair for the latter.

Figure 8 shows frequency responses calculated for the actuated suspensions under the sinusoidal voltage supplies at 30 V. The responses are the amplitude of velocity, taken at the tip or the dimple point of the suspensions. It is observed that the inline-actuated suspensions have lower velocity amplitudes, as compared to the push–pull actuated suspension. However, the inline designs improve the sway frequency. The inline actuator, which is lapped with a piezoelectric plate on one side, is observed to have two spikes of vibration below the main sway resonance at 10 kHz. The first spike is a coupled mode at a low frequency. The coupled mode is attributed to in-plane asymmetry due to mounting locations that couples bending and torsional at the lower frequency. The second is a torsional mode at about 6 kHz.

The thickness asymmetry, due to a single-sided lapping of the piezoelectric plate, introduces a torsional unbalance to the suspension assembly. Fortunately, the thickness asymmetry can be reduced by lapping two pieces of piezoelectric plates from both sides of the load beam. Figure 8 shows that the frequency response of the both-sided lapping is smoother than that of the one-sided lapping. Moreover, there is an alternative approach to reduce the thickness asymmetry: lowering the plane of mounting tabs so that the neutral plane of the piezoelectric plate is aligned with that of the load beam. This approach will be studied in a subsequent work.

3.3. Parametric study

An actuating mechanism generally weakens the structure of a suspension. Stiffening the mechanism could mitigate its adverse influence on suspension dynamics, but it reduces

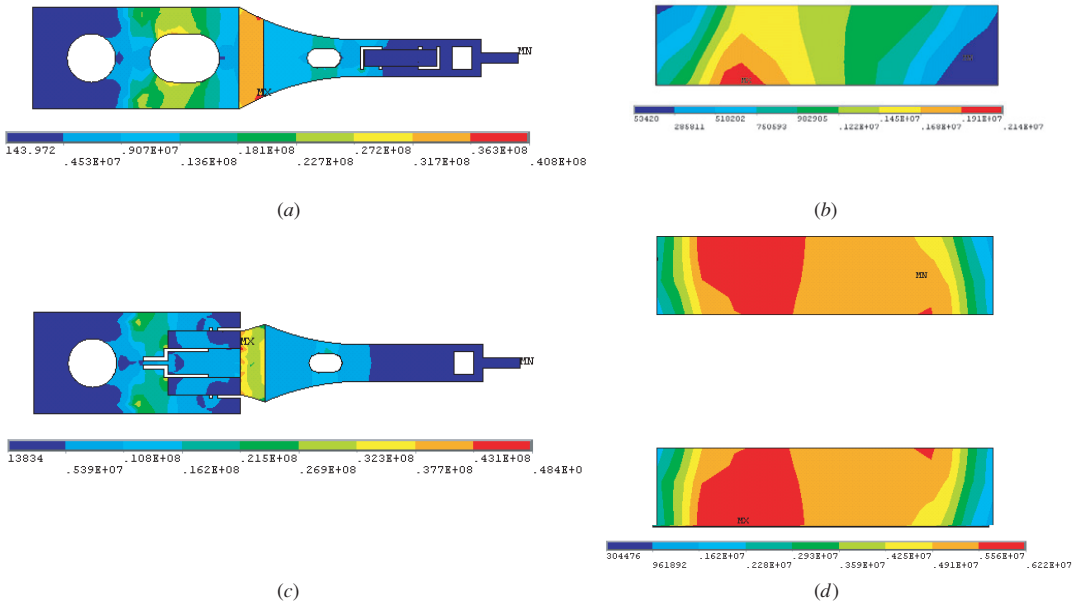

Figure 6. Stress distribution under an out-of-plane static acceleration of 100 G: (*a*) on an inline-actuated suspension and (*b*) on the inline piezoelectric plate; (*c*) on a push–pull actuated suspension and (*d*) on the pair of push–pull piezoelectric plates.

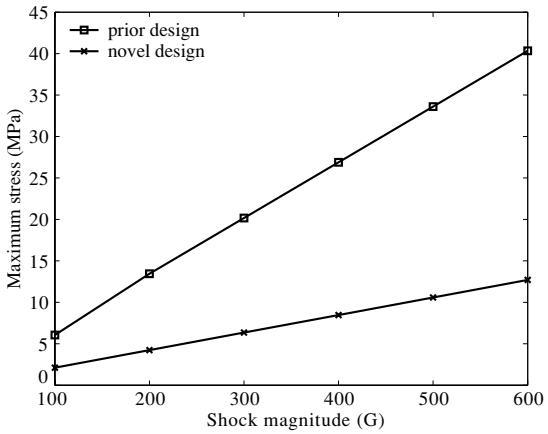

Figure 7. Maximum stress imparted to the piezoelectric plate of actuated suspensions under shock acceleration.

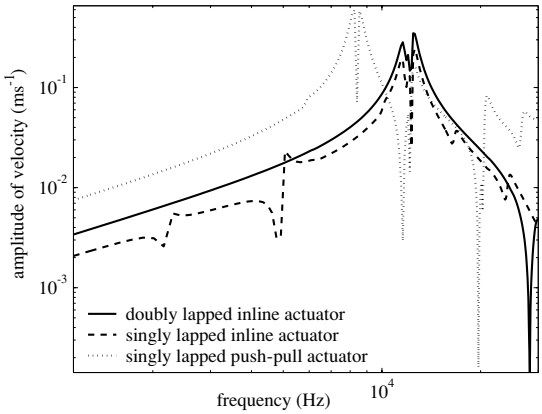

Figure 8. Frequency response of the actuated suspensions: amplitude of the lateral velocity at tip over the range of driving frequencies.

the capability to generate the actuation stroke as well. The inline actuation mechanism does influence the suspension dynamics because it is configured at the elongated portion of the suspension structure. Two design parameters are found to be critical to the static and dynamic performances of the actuated suspension. They are the length and the width of the actuation mechanism. Like the suspension width of the elongated portion (figure 3), the hinge width of the parallel mechanism could affect torsional and sway frequencies of the suspension assembly [14]. On the other hand, the length of the parallel mechanism mainly affects the sway frequency.

Using a standard bulk piezoelectric plate (3 mm long, 0.7 mm wide), the dimensions of the parallel mechanism are roughly restricted within a narrow design domain. The design parameter that remains tunable is actually the hinge width. The hinge width and the piezoelectric plate width basically define the end width of the suspension. An increase in the hinge width results in an increase in the suspension width. Hence, it is expected to have an influence on the suspension performance.

Figure 9 shows influences of the hinge width on static and dynamic responses of the suspension assembly. It is observed that a lateral stroke decreases with the increasing hinge width (figure 9(*a*)), whereas the maximum stress of piezoelectric plate under shock acceleration generally decreases with the increasing hinge width (figure 9(*b*)). Figure 9(*c*) shows that spring rate increases with the increasing hinge width at decreasing rate. On dynamic responses, the first torsional frequency and cantilever frequency decrease with the increasing hinge width but the first sway frequency increases with it as shown in figure 9(*d*). With the knowledge of the performance trends, one can embody a wider hinge in a load beam design to achieve a higher sway frequency and a high shock resistance.

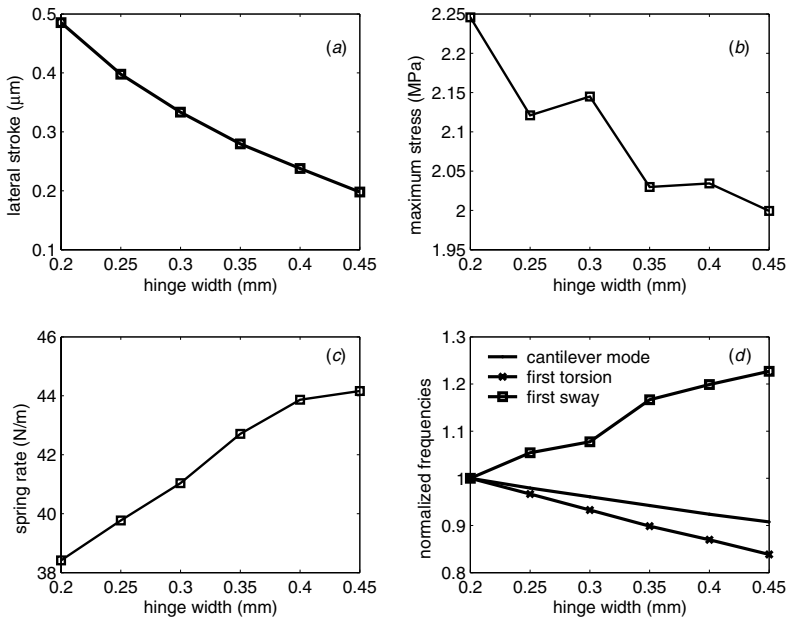

Figure 9. Trends with respect to hinge width for an inline-actuated suspension with a 0.1 mm thick piezoelectric plate: (*a*) lateral stroke; (*b*) maximum stress in the piezoelectric plate; (*c*) spring rate; (*d*) normalized frequencies.

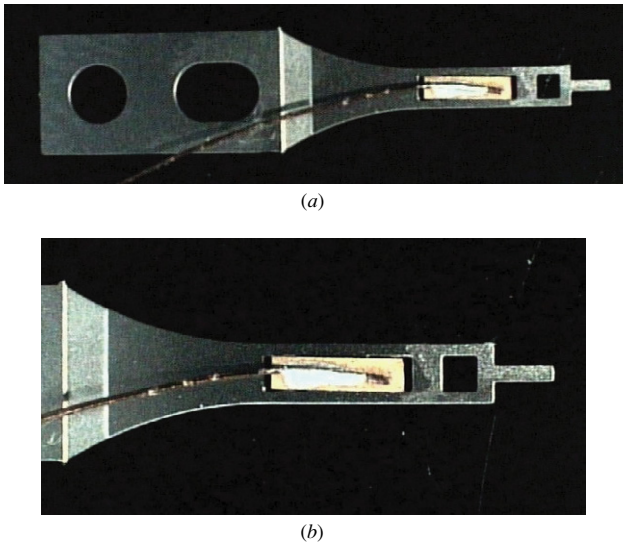

Figure 10. A fabricated and assembled prototype of the inline-actuated suspension: (*a*) full view; (*b*) zoomed view.

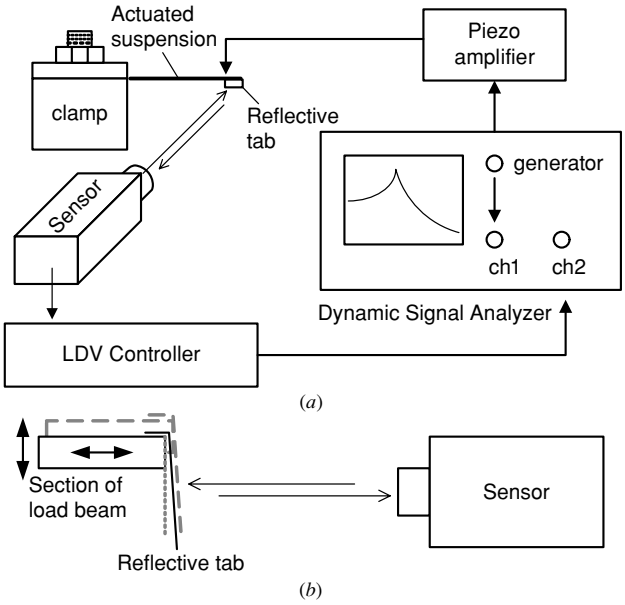

Figure 11. Schematic showing (*a*) the experiment set-up used for measuring the velocity amplitude of a self-driven in-line actuated suspension; (*b*) possible deviation in measuring the in-plane velocity as the suspension vibrates in-plane and out-of-plane simultaneously during actuation.

4. Experiments

4.1. Prototype

A prototype of the inline-actuated suspension is fabricated. Its load beam is made of stainless steel foil of 0.10 mm thick and their shape is formed using photochemical machining. A bulk piezoelectric plate is bonded with an electrode surface on top of the mounting tabs using conductive adhesive. Another free electrode surface of the piezoelectric plate is connected to a copper wire. The assembly is done manually with the help of tweezers and an optical microscope, and it is fixed using adhesive bonding, which is cured on a hot plate. Figure 10 shows the finished assembly of the inline-actuated suspension.

4.2. Measurement

Figure 11(*a*) shows a schematic of the experiment set-up used to measure the in-plane velocity amplitude of the actuated suspension. In the set-up, the suspension is clamped at its base plate using a stainless-steel clamp holder. The bottom electrode surface of the plate, together with the load beam, is grounded through the clamp holder while the top electrode surface is supplied with 30 V through the copper wire. A reflective tab (see figure 11(*b*)) is adhered to the tip of the

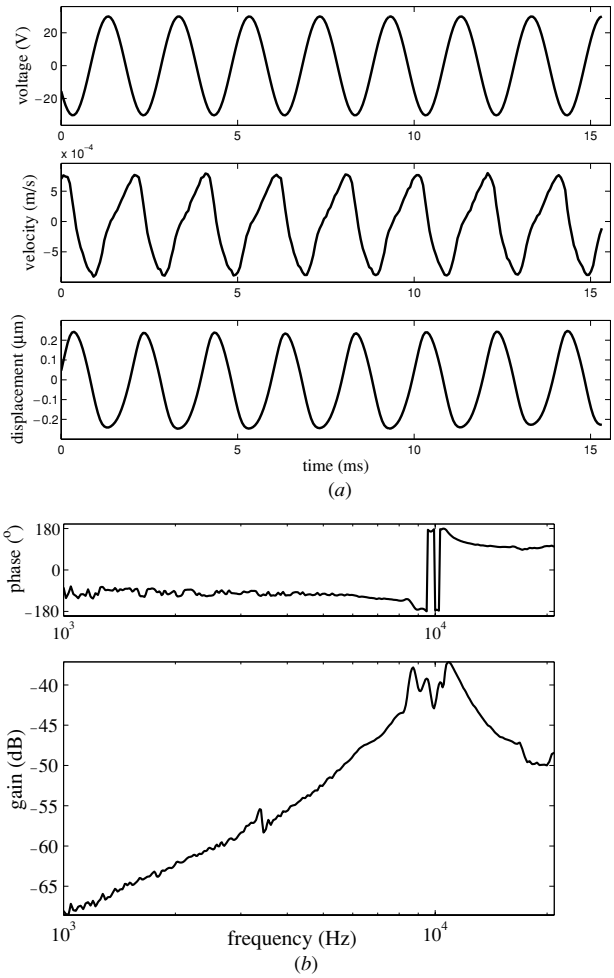

Figure 12. Lateral stroke measured for the inline-actuated suspension: (*a*) harmonic responses under 500 Hz excitation showing driving voltages, measured velocity and numerically derived displacement; (*b*) frequency response ranging from 1 kHz to 25 kHz.

suspension. Such a tab is needed because the sidewall of the suspension is too thin and too rough to properly reflect a laser light shot for an in-plane velocity measurement. The system used for velocity measurement is a Polytec scanning laser Doppler vibrometer. With the set-up, the actuated suspension is self-driven into vibration. The measured sensor signal and the input signal are fed into a dynamic signal analyser to display the frequency responses during the modal testing.

Mechanical responses of the inline-actuated suspension are tested. Figure 12(*a*) shows the 500 Hz 30 V sinusoidal input voltage applied to the actuated suspension. It shows the in-plane velocity measured at the reflective tab, with an obvious hysterisis between the increasing voltages and the decreasing voltages. In addition, the maximum velocity amplitude is observed to deviate from the minimum velocity amplitude. The deviation is possibly attributed to the imperfect structure and an unintended out-of-plane motion. As the suspension is actuated, the unintended out-of-plane motion is produced together with the intended in-plane motion. Hence, the reflective tab at which the laser shot is moving out-of-plane and in-plane simultaneously. During the in-plane velocity measurement, the simultaneous out-of-plane motion may be measured with an in-plane component when the laser is scanning over the small-area topography of the moving reflective tab, rather than shooting at the fixed material spot on it.

The deviation between the maximum and the minimum velocity amplitudes results in a net motion over a cycle when it is integrated numerically. However, the net motion is not possible because the actuator should always return to the starting position after a cycle. The net motion is possibly caused by repeatable errors in measurement over the moving topography on the reflective tab. If the net motion is zero, the numerically derived harmonic motion can be leveled to give an estimate on the in-plane actuation. Based on this assumption, a harmonic lateral displacement at tip under 30 V and 500 Hz is derived to have a stroke amplitude of 0.24 μm (figure 12(*a*)). It is also understood that the discrepancy between the measured and the predicted strokes may also be attributed to dimensional deviation of adhesive thickness and flexural width of parallel beams for the suspension, besides the measurement errors mentioned.

Figure 11(*b*) shows the frequency response of the inline-actuated suspension, sweeping from 1 kHz to 25 kHz. In general, the measured frequency response agrees in trend with the predicted response obtained from finite element simulation. However, the measured resonances deviate from the predicted values to certain extent. The first torsional frequency is measured around 3 kHz. It is much lower than the predicted 6.24 kHz. The deviation may arise due to the fact that the copper wire attached to the top electrode deteriorates the thickness asymmetry. The second torsional and the first sway frequencies occur around 8 kHz and 10 kHz, which are slightly smaller than the predicted values.

5. Conclusion

This paper describes a novel design concept of an inline-actuated suspension using a piezoelectric element to drive a parallel mechanism into a lateral stroke. The design is fit into an elongated portion of a slender load beam and is deployed closer to the magnetic head. The compact design can produce an adequate stroke and achieve enhanced dynamic performances, in particular, the high sway frequency and the high shock resistance. These performance enhancements are achieved without resorting to costly miniaturization of piezoelectric elements. The present design of actuated suspension can be realized using a standard manufacturing process, without incurring an additional manufacturing overhead.

Acknowledgments

This project was done when the first author was working with the Center for Mechanics of Micro-Systems (CMMS), Nanyang Technological University, Singapore. The authors would like to acknowledge Dr Guo G X and Dr Ong E H of the Data Storage Institute, Singapore for valuable discussion. The authors also would like to thank Mr Cheo H L and Mrs Halimatun for laboratory support.

References

[1] Nakamura S, Numasato H, Sato K, Kobayashi M and Naniwa I 2002 A push–pull multi-layered piggyback PZT actuator *Microsyst. Technol.* **8** 149–54

[2] Mori K, Munemoto T, Otsuki H, Yamaguchi Y and Akagi K 1991 A dual-stage magnetic disk drive actuator using a piezoelectric device for a high track density *IEEE Trans. Magn.* **27** 5298–300

[3] Evans R B, Griesbach J S and Messner W C 1999 Piezoelectric microactuator for dual stage control *IEEE Trans. Magn.* **35** 977–82

[4] Tokuyama M, Shimizu T, Masuda H, Nakamura S, Hanya M, Iriuchijima O and Soga J 2001 Development of a phi-shaped actuated suspension for 100-kTPI hard disk drives *IEEE Trans. Magn.* **37** 1884–6

[5] Koganezawa S, Uematsu Y, Yamada T, Nakano H, Inoue J and Suzuki T 1998 Shear mode piezoelectric microactuator for magnetic disk drives *IEEE Trans. Magn.* **34** 1910–2

[6] Koganezawa S, Takaishi K, Mizoshita Y, Uematsu Y, Yamada T, Hasegawa S and Ueno T 1996 A flexural piggyback milli-actuator for over 5 Gbit/in.2 density magnetic recording *IEEE Trans. Magn.* **32** 3908–10

[7] Koganezawa S, Hara T, Uematsu Y and Yamada T 2001 Effect of dual-stage actuator on positioning accuracy in 10 k rpm magnetic disk drives *IEEE Trans. Magn.* **37** 955–8

[8] Shimizu H, Shimizu T, Tokuyama M, Masuda H and Nakamura S 2003 Numerical simulation of positioning error caused by air-flow-induced vibration of head gimbals assembly in hard disk drive *IEEE Trans. Magn.* **39** 806–11

[9] Shimizu H, Tokuyama M, Imai S, Nakamura S and Sakai K 2001 Study of aerodynamic characteristics in hard disk drives by numerical simulation *IEEE Trans. Magn.* **37** 831–6

[10] Lau G K and Du H 2005 Topology optimization of head suspension assemblies using modal participation factor for mode tracking *Microsyst. Technol.* **11** 1243–51

[11] Du H J, Lau G K and Liu B 2005 Actuated suspensions with enhanced dynamics for hard disk drives *IEEE Trans. Magn.* **41** 2887–9

[12] Fuji Ceramics 1999 *The Table for Piezo Ceramic Material Constants* (Tokyo: Fuji Ceramic Corporation)

[13] Loctite 1998 *Technical Data Sheet for Product 3880* (Dublin, Ireland: Loctite Research, Development and Engineering)

[14] Lau G K, Qi G, Primanti A, Liu F and Du H 2004 An integral flexure for rotary actuators in hard disk drives *Sensors Actuators* A **113** 116–24